Vol.69: e26250567, 2026
https://doi.org/10.1590/1678-4324-2026250567
ISSN 1678-4324 Online Edition

BABT
Brazilian Archives of Biology and Technology

Article - Biological, Medical and Health Technologies

Green Synthesis of Silver Nanoparticles Using Hexane Extract from *Pterodon pubescens* Benth. and their Antibacterial Activity and Biocompatibility Evaluation

Jaciel Gonçalves dos Santos[1]
https://orcid.org/0000-0002-7143-5015

Cassia Cristina Fernandes[1]
https://orcid.org/0000-0003-2004-3166

Adriano Jakelaitis[1]
https://orcid.org/0000-0003-0093-9846

Mariana Brentini Santiago[2]
http://orcid.org/0000-0002-6060-379X

Carlos Henrique Gomes Martins[2]
https://orcid.org/0000-0001-8634-6878

Matheus Reis Santos de Melo[3]
https://orcid.org/0000- 0001-5475-2492

Denise Crispim Tavares[3]
https://orcid.org/0000-0003-4646-5914

Mayker Lazaro Dantas Miranda[4*]
https://orcid.org/0000-0003-4689-572X

[1]Instituto Federal de Educação, Ciência e Tecnologia Goiano, *Campus* Rio Verde, Rio Verde, GO, Brasil; [2]Universidade Federal de Uberlândia, Instituto de Ciências Biomédicas, Departamento de Microbiologia, Uberlândia, MG, Brasil. [3]Universidade de Franca, Franca, SP, Brasil. [4]Instituto Federal de Educação, Ciência e Tecnologia de Mato Grosso do Sul, *Campus* Campo Grande, Campo Grande, MS, Brasil.

Editor-in-Chief: Paulo Vitor Farago
Associate Editor: Jane Manfron

Received: 17-Jul-2025; Accepted: 26-Jan-2026

*Correspondence: mayker.dantas@ifms.edu.br; Tel. no.: +55-67-99289-5657 (M.L.D.M)

HIGHLIGHTS

- Active silver nanoparticles (AgNPs) were prepared using hexane extract from *P. pubescens* seeds (HE-PP).
- HE-PP-mediated silver nanoparticles showed potent activity against oral, phytopathogenic, *H. pylori* and mycobacterial strains.
- Consistent antibacterial activities were observed regardless of bacterial resistance profiles.
- FTIR analysis confirmed reduction of silver ions by bioactive plant compounds.
- Nanoparticles showed favorable selectivity toward bacteria over human cells.

Abstract: The growing problem of microbial resistance to conventional antimicrobials has intensified the search for sustainable alternatives, including metallic nanoparticles produced by green chemistry. In this study, silver nanoparticles (AgNPs) were synthesized using the hexane extract from *Pterodon pubescens* seeds (HE-PP), a source rich in terpenoids and bioactive compounds that act as natural reducing and stabilizing agents. Nanoparticle formation was confirmed by UV–Vis spectroscopy and scanning electron microscopy, which revealed predominantly spherical particles. Complementary analyses indicated an average hydrodynamic size of 187.4 ± 12.6 nm with a moderate polydispersity index (PDI = 0.234), negative zeta potential (–31.6 ± 1.4 mV), and a high synthesis yield, while elemental characterization confirmed silver

as the major component. The nanoparticles remained colloidally stable for at least 30 days. The antibacterial potential of HE-PP-mediated AgNPs was assessed against clinically relevant and phytopathogenic strains (MIC range 0.48-25 µg/mL). Strong activity was observed against oral pathogens (*P. gingivalis, P. nigrescens, A. naeslundii, A. actinomycetemcomitans, B. fragilis, and P. anaerobius*), phytopathogenic *Xanthomonas citri* (MIC = 0.48 µg/mL), *Helicobacter pylori* (MIC = 25 µg/mL), and mycobacteria (*M. tuberculosis, M. avium,* and *M. kansasii*; MIC = 7.8 µg/mL). Importantly, cytotoxicity evaluation in normal human fibroblasts (GM07492A cells) revealed reduced cell viability only at concentrations higher than those required for antibacterial activity (IC_{50} = 62.56 ± 3.38 µg/mL), indicating a favorable preliminary selectivity profile. Overall, HE-PP-mediated AgNPs demonstrated robust physicochemical properties, significant antibacterial efficacy, and promising selectivity, highlighting their potential as eco-friendly antimicrobial agents. This study reinforces the role of *P. pubescens* as a sustainable source for nanomaterial development and expands the scope of phytochemical-mediated nanotechnology for biomedical and agricultural applications.

Keywords: Nanobiotechnology; material science; medicinal plants; *sucupira-branca*.

INTRODUCTION

Pterodon pubescens Benth., commonly known as "*sucupira-branca*," is a tree species native to the Brazilian *Cerrado* and belongs to the Fabaceae family. This species is traditionally used in folk medicine for its anti-inflammatory and analgesic properties, and has attracted increasing scientific interest due to its pharmacological potential and rich diversity of bioactive compounds [1]. A recent study has reported significant biological activities from extracts obtained from its seeds, leaves, and fruits, particularly in microbiology, oncology, and neuropharmacology [2].

The chemical composition of *P. pubescens* is characterized by a high terpenoid content, including vouacapane-type diterpenes such as 6α-acetoxy-7β-hydroxy-vouacapan-17β-oate methyl ester, and sesquiterpenes such as *E*-caryophyllene and γ-muurolene [3]. These compounds are believed to be primarily responsible for the plant's pharmacological activities, acting as anti-inflammatory, antioxidant, and antimicrobial agents [4]. Phytochemical analyses have shown that the hexane extract from the seeds contains a rich oleaginous fraction with both volatile and non-volatile constituents that exhibit potent bioactivity [1].

The biological applications of *P. pubescens* have been extensively investigated. *Sucupira* extracts have demonstrated significant antimicrobial activity against various bacterial strains, including *Mycobacterium tuberculosis* and oral pathogens such as *Porphyromonas gingivalis*, with minimum inhibitory concentrations (MICs) ranging from 12.50 to 500 µg/mL [1]. In addition, antiproliferative activity has been observed in several cancer cell lines, including leukemia, melanoma, and prostate cancer cells, with these effects attributed to the ability of its terpenes to modulate cell signaling pathways and regulate genes involved in the cell cycle and apoptosis [2,5,6].

Pharmacological studies have also shown that *P. pubescens* exhibits strong antinociceptive and anti-inflammatory properties capable of reducing nociceptive responses in animal models of acute and chronic pain [3,4]. These effects are thought to be mediated by modulation of the glutamatergic system and inhibition of inflammatory cytokines such as TNF-α and IL-1β [4]. Toxicological assessments indicate that while high doses may lead to hepatic alterations, moderate concentrations of extracts and isolated fractions are generally safe for therapeutic use [7]. Altogether, these findings highlight the potential of *P. pubescens* as a promising source for the development of phytotherapeutics and bioactive nanomaterials.

The use of plant extracts in the green synthesis of silver nanoparticles (AgNPs) represents a promising and rapidly expanding research field within nanobiotechnology [8]. This eco-friendly approach harnesses the natural reducing and stabilizing capabilities of phytochemicals, allowing to produce nanoparticles under mild conditions and without the need for hazardous reagents [9]. The resulting AgNPs often exhibit enhanced biological properties, particularly antimicrobial activity, due to the synergistic interaction between silver ions and plant-derived compounds [9]. Given the versatility, sustainability, and growing applicability of this method in the development of bioactive nanomaterials, the present study employed the hexane extract from *Pterodon pubescens* (HE-PP) to synthesize AgNPs, aiming to explore its potential as a natural and effective antibacterial agent in green nanotechnology.

Considering the growing concern regarding antimicrobial resistance and the need for sustainable alternatives, this study aims to contribute to advance green nanotechnology by synthesizing silver nanoparticles using HE-PP. The novelty of this work lies in the unprecedented use of HE-PP as a natural reducing and stabilizing agent in formulating AgNPs. A diverse panel of bacterial strains was tested to assess the antimicrobial potential of the synthesized nanoparticles, including periodontopathogenic,

phytopathogenic, and mycobacterial species, offering a broad perspective on their biological applicability. The nanoparticles were characterized using UV-Vis spectroscopy to confirm their formation and surface plasmon resonance, as well as scanning electron microscopy to determine their morphology and size distribution. Together, these evaluations provide a comprehensive understanding of the physicochemical properties and bioactivity of HE-PP-mediated AgNPs, reinforcing their potential as innovative agents in the control of resistant microbial pathogens.

MATERIAL AND METHODS

Plant material

First, 300 g of *P. pubescens* seeds were collected on November 2nd, 2022, in Unit I at the Universidade Federal de Mato Grosso (UFMT), Campus Universitário do Araguaia (CUA), Pontal do Araguaia, Mato Grosso (MT) state, Brazil (15°55'08.4"S 52°16'42.9"W) – Figure 1. Taxonomic identification was performed by the biologist Maryland Sanchez Lacerda and an exsiccate (no. 1950) was deposited at the herbarium belonging to the UFMT-CUA. Seeds were washed with distilled water and dried at room temperature (25°C). After complete drying, the plant material was stored in a sealed container in a dark cool place. Access to the botanical material was approved by the *Sistema Nacional de Gestão do Patrimônio Genético e do Conhecimento Tradicional Associado* (*SISGEN*) under the code AEACDCA.

Figure 1. *Pterodon pubescens* Benth. in its natural habitat and morphological characteristics of its fruits. (**1**) Adult specimens of *P. pubescens* in a *Cerrado* area; (**2**) Harvesting process of fruits directly from the tree canopy; (**3**) Detail of the fruits used for preparing the hexane extract (HE-PP) employed in the green synthesis of silver nanoparticles.

Preparation of hexane extract from *P. pubescens seeds* (HE-PP)

The methodology proposed by Batalini and coauthors (2020) [10], with minor modifications, was used for preparing HE-PP. Whole seeds (300 g; solid/liquid ratio 0.75 g/mL) were macerated in 400 mL of hexane at room temperature in an amber glass flask kept in the dark for 15 days. After extraction, the mixture was filtered to separate plant material from the solvent, which was recovered by rotary evaporation under reduced pressure. The crude hexane extract was dried in an oven at 38 °C for 48 h until constant weight. The HE-PP (5 g; 1.66% w/w) was stored in amber bottles at 4 °C until analysis.

Chemical identification of hexane extract from *P. pubescens seeds* (HE-PP)

HE-PP was dissolved in ethyl ether and analyzed by gas chromatography-flame ionization detection (GC-FID) and gas chromatography-mass spectrometry (GC-MS) using Shimadzu QP5000 Plus and GCMS2010 Plus (Shimadzu Corporation, Kyoto, Japan) systems. The temperature of the column in GC-FID was programmed to rise from 60 to 240°C at 3°C/min and was held at 240°C for 5 min; the carrier gas was H_2 at the flow rate of 1.00 mL/min. The equipment was set to operate in the injection mode; the injection volume was 0.1 µL (split ratio of 1:10), while injector and detector temperatures were 240 and 280°C, respectively. Relative concentrations of components were obtained by normalizing peak areas (%). Relative areas consisted of the average of triplicate GC-FID analyses. GC-MS conditions and the identification have been previously reported [11]. Identification of volatile components of HE-PP was based on their retention indices on an Rtx-5MS (30 m X 0.25 mm; 0.250 µm) capillary column under the same operating conditions used for GC relative to a homologous series of *n*-alkanes (C_8-C_{20}). Structures were computer-matched with Wiley 7, NIST 08 and FFNSC 1.2 and their fragmentation patterns were compared with literature data [12].

Synthesis of silver nanoparticles

A 0.01 mol/L silver nitrate ($AgNO_3$) solution was prepared and utilized for the synthesis of silver nanoparticles (AgNPs). Prior to nanoparticle synthesis, the HE-PP extract was filtered through sterile Whatman No. 1 filter paper to remove particulate material. Although not sterilized, the extract was handled under aseptic conditions, following procedures commonly reported in green-synthesis methodologies. Subsequently, 1 g of the filtered HE-PP was dissolved in 5 mL of absolute ethanol and heated to 60 °C under constant stirring. After 15 minutes, 5 mL of the $AgNO_3$ solution was added to the mixture, and the reaction was maintained under the same conditions for an additional 60 minutes. The formation of AgNPs was preliminarily indicated by a visible color change in the reaction medium, consistent with surface plasmon resonance phenomena observed in green synthesis protocols [13]. The final concentration of AgNPs in the colloidal suspension was 18.4 ± 1.2 mg/mL, as determined by ICP-OES. The freshly synthesized AgNP suspension presented a pH of 9, in accordance with values typically observed in phytochemical-based AgNP preparations. The reaction was conducted under light-protected conditions to avoid premature photoreduction of Ag^+, following procedures reported in similar green-synthesis studies.

Characterization of HE-PP-mediated AgNPs

The synthesized AgNPs were characterized using Transmission Electron Microscopy (TEM) with a JEM-2100 (JEOL) microscope operating at an accelerating voltage of up to 200 kV. Samples were prepared by depositing the colloidal suspension onto copper grids coated with formvar and carbon films, enabling assessment of the nanoparticle morphology and size distribution [14]. Additionally, Fourier Transform Infrared Spectroscopy (FTIR) was performed using a Jasco FT/IR-4100 spectrometer in the range of 4000–400 cm^{-1}. KBr pellets containing AgNPs and HE-PP were analyzed to identify functional groups involved in the reduction and stabilization of the nanoparticles. The FTIR spectra revealed characteristic peaks corresponding to phenolic and carbonyl groups, indicating the role of phytochemicals in capping and stabilizing the AgNPs [15]. The average hydrodynamic diameter, polydispersity index (PDI), and zeta potential of the nanoparticles were measured using a Zetasizer® Nano ZS90 (Malvern Instruments, Malvern, UK). The colloidal suspension was diluted in ultrapure water at a 1:500 ratio and analyzed in triplicate at 25 °C. The zeta potential was used as an indicator of colloidal stability, with values above ±30 mV considered indicative of electrostatic stabilization. The pH of the nanoparticle suspension was measured immediately after synthesis using a calibrated digital potentiometer (Digimed®, São Paulo, Brazil) with buffer solutions of pH 4.0 and 9.0. Visual observation of the colloidal dispersion was performed for 30 days at room temperature to assess sedimentation and aggregation as indirect evidence of colloidal stability. The synthesis yield was calculated gravimetrically based on the difference between the initial amount of silver nitrate ($AgNO_3$) used and the mass of dried nanoparticles obtained after purification and drying at 38 °C. The yield was expressed as a percentage. The elemental composition of the nanoparticles was determined by energy-dispersive X-ray spectroscopy (EDX) coupled with scanning electron microscopy (SEM, JEOL JSM-6510LV, Japan). The EDX spectra were used to confirm the presence of silver as the major element, along with possible traces of carbon and oxygen from phytochemicals associated with nanoparticle surface capping. Alternatively, samples were also analyzed by inductively coupled plasma optical emission spectrometry (ICP-OES, PerkinElmer Optima 8000, USA) to quantify total silver content in the nanoparticle suspension, expressed in mg/L. All measurements were performed in triplicate. Statistical analysis was conducted using one-way analysis of variance (ANOVA), followed by Tukey's post hoc test with GraphPad Prism® version 6.01 (GraphPad Software, San Diego, CA, USA). A significance level of $p < 0.05$ was adopted.

Anti-periodontopathogenic assay of HE-PP-mediated AgNPs

This biological assay was guided by the current methodology proposed by Santos and coauthors (2025) [16]. The following periodontopathogenic bacterial strains from the American Type Culture Collection (ATCC) were employed to conduct assays of antibacterial and antibiofilm activities: *Porphyromonas gingivalis* (ATCC 33277), *Fusobacterium nucleatum* (ATCC 25586), *Prevotella nigrescens* (ATCC 33563), and *Actinomyces naeslundii* (ATCC 19039), *Aggregatibacter actinomycetemcomitans* (ATCC 43717), *Bacteroides fragilis* (ATCC 25285) and *Peptostreptococcus anaerobius* (ATCC 27337).

Antibacterial activity of HE-PP was evaluated by the broth microdilution method, in triplicate. Assays were conducted on 96-well microplates. The inoculum was standardized to the McFarland 0.5 scale and diluted to bacterial concentration of 1.5×10^6 CFU/mL in the wells. In order to prepare the samples, HE-PP-mediated AgNPs was solubilized in 5% dimethyl sulfoxide (DMSO) and diluted in Brucella broth supplemented with hemin (5.0 mg/mL) and menadione (1.0 mg/mL); a twofold serial dilution at concentrations ranging from 0.195 to 400 µg/mL was used. Control of 5% DMSO was performed and the solvent did not interfere with bacterial growth at this concentration. Chlorhexidine was used as the positive control at concentrations ranging from 0.115 to 5.9 µg/mL. The following controls were also performed: inoculum (all bacteria used in the assay + the culture medium), to observe bacterium viability; broth, to ensure that the culture medium is sterile; and a HE-PP-mediated AgNP sample to guarantee that this solution is sterile. Microplates were incubated in an anaerobic chamber (Don Whitley Scientific, Bradford, U.K.) under anaerobic conditions (80% N_2, 10% CO_2 and 10% H_2) at 37°C for 72 h. Resazurin was used for revealing bacterial growth, i.e. blue meant the absence of bacterial growth, while pink showed the presence of bacteria.

Antimycobacterial assay of HE-PP-mediated AgNPs

The following ATCC and clinical isolates were used and maintained at -80°C to evaluate antimycobacterial activity: *M. tuberculosis* H37Rv (ATCC 27294), *M. kansasii* (ATCC 12478) and *M. avium* (ATCC 25291).

Minimum inhibitory concentration (MIC) was determined by microdilution on a microplate to evaluate the antimycobacterial activity of samples. Resazurin was used for revealing bacterial growth by the Resazurin Microtiter Assay (REMA). The experiment was conducted in triplicate. HE-PP-mediated AgNPs were dissolved in DMSO and serially diluted in Middlebrook 7H9 broth (Difco, Sparks, MD, USA) before inoculation. HE-PP-mediated AgNP concentrations ranged from 3.90 to 500 µg/mL, while final DMSO (Sigma-Aldrich, St. Louis, MO, USA) content in the assay was below 0.3%. Isoniazid (Sigma-Aldrich) was used as the reference antibiotic drug at concentrations ranging from 0.015 to 1.0 µg/mL. The inoculum was prepared by introducing a range of colonies grown in Ogawa–Kudoh (LaborClin, Pinhais, PR, Brazil) in a tube containing glass beads with 500 µL sterile water. A 200-µl aliquot was transferred to a tube with 2 ml 7H9 broth (Difco), incubated at 37°C for 7 days and then compared with McFarland scale 1. After the inoculum was standardized, it was diluted with 7H9 broth (Difco) in the ratio of 1:25. Growth controls containing no antibiotics and sterility controls without inoculation were also included. Plates were incubated at 37°C for 7 days. Then, 30 µL 0.02% Resazurin (Sigma-Aldrich) aqueous solution was added to each well. After standing for 18 h, the visual MIC was defined as the lowest sample concentration that was able to inhibit growth of mycobacterium strains [16].

Anti-Xanthomonas citri assay of HE-PP-mediated AgNPs

The bacterium *Xanthomonas citri* subsp. *citri* (*X. citri* isolated 12, sensitive to copper; *X. citri* isolated 1733, tolerant to copper and *X. citri* isolated 1647, resistant to copper) was grown in Nutrient Agar (NA) or Nutrient Broth (NB) and incubated at 28°C for 72 h. All strains were supplied by the Fund for Citrus Protection (FUNDECITRUS) in Araraquara, SP, Brazil.

MIC is the lowest concentration of HE-PP-mediated AgNPs that was able to inhibit bacterium growth. It was determined by using the broth microdilution method on 96-well culture plates [17]. Samples were first dissolved in 5% DMSO and then diluted in NB to reach concentrations ranging from 0.98 to 2.000 µg/mL. Inoculums were adjusted to produce final cell concentration of 5×10^5 CFU/mL. Streptomycin was used as the positive control at concentrations ranging from 0.0115 to 5.9 µg/mL. Plates were incubated in Biochemical Oxygen Demand (BOD) at 28°C for 72 h. After incubation, 30 µL Resazurin aqueous solution at 0.02%, used as the bacterial revelator, was placed into each well. Plates were incubated again at 28°C for 12 h. Wells that became pink exhibited bacterial growth, while those that remained blue showed that there was inhibition. Three independent experiments were performed in triplicate.

Anti-H. pylori assay of HE-PP-mediated AgNPs

Minimum inhibitory concentration (MIC in µg/mL) of HE-PP-mediated AgNPs was calculated by the broth microdilution method on 96-well microplates using the *Helicobacter pylori* (ATCC 43526) ATCC reference strain. The HE-PP-mediated AgNP activity with reference drugs was evaluated by comparing bacterial growth on each plate of *H. pylori*. HE-PP-mediated AgNPs were dissolved in 5% DMSO to reach final concentrations ranging between 0.195 and 400 µg/mL. The inoculum was adjusted at 625 nm in a spectrophotometer to produce a cell concentration equal to 5 x 10^5 CFU/mL. Plates were incubated in a CO_2 incubator at 37°C for 3 days under microaerobic conditions. Tetracycline, at concentrations ranging from 0.115 to 59.0 µg/mL, was employed as the standard drug and incubated under the previously mentioned conditions. After incubation, 30 µL 0.01% aqueous resazurin solution was added to each well to evaluate microbial growth [18].

Biocompatibility evaluation

Biocompatibility evaluation was performed using the resazurin colorimetric assay, according to Riss and coauthors [19]. For the experiments, 1x10^4 human fibroblasts (GM07492A cells) were seeded in 96-well microplates. The HE-PP-mediated AgNPs was initially dissolved in DMSO and then diluted in complete medium, with concentrations ranging from 1.95 to 250 µg/mL. Each plate contained wells for negative (no treatment), solvent (1% DMSO), and positive (25% DMSO) controls. After a 24-h incubation period at 36.5 °C, the culture medium was aspirated, and the cells were washed with phosphate-buffered saline to remove treatments before being exposed to 80 µL of Ham's Nutrient Mixture F10 culture medium without phenol red (Sigma-Aldrich). Subsequently, 20 µL of resazurin (0.03 mg/mL) was added to each well, followed by a new incubation at 36.5 °C for 4 hours. Absorbance was measured at 570 nm (with a reference at 600 nm) using a multi-plate reader (Asys – UVM 340, Microwin 2.000 program). Nonlinear regression analysis was conducted using GraphPad Prism software to determine the concentration of HE-PP-mediated AgNPs that inhibited 50% of cell viability (IC_{50}).

RESULTS AND DISCUSSION

The decision to incorporate hexane extract from *P. pubescens* seeds (HE-PP) into silver nanoparticles (AgNPs) stems from promising results obtained in our previous study [16], which demonstrated significant antibacterial activity of the extract against a wide range of pathogenic and phytopathogenic bacteria. These findings highlighted the biological potential of HE-PP, with MIC values as low as 12.50 µg/mL against oral pathogens and notable effects against *M. tuberculosis*, *X. citri*, and other clinically relevant strains. Building upon these results, the present work aims to advance the investigation by developing HE-PP-mediated AgNPs and evaluate their antimicrobial performance against a broader bacterial panel. In addition, we characterized the physicochemical properties of the nanoparticles to better understand their potential as innovative agents in combating resistant microbial pathogens.

The phytochemical analysis of HE-PP conducted by Santos and coauthors [16] revealed that its biological activity is likely attributed to four major constituents: *E*-geranylgeraniol, dehydroabietol, *E*-caryophyllene, and vouacapane-type diterpenes. These compounds are well-documented in the literature for their potent antibacterial, anti-inflammatory, and cytotoxic properties [20]. Notably, *E*-geranylgeraniol has demonstrated pro-apoptotic activity in cancer cells and strong antimicrobial potential, while dehydroabietol and vouacapane diterpenoids are associated with significant bioactivity against resistant microbial strains [21-22]. The incorporation of these phytochemicals into AgNPs is expected to enhance their bioavailability and therapeutic performance, providing a synergistic antimicrobial effect through the combined action of silver ions and plant-derived bioactives [23]. Thus, this study explores the convergence of phytochemistry and nanotechnology as a promising strategy to address bacterial resistance.

Although the chemical characterization of the hexane extract of *P. pubescens* was primarily aimed at identifying its major volatile constituents, the classes of compounds detected also provide important insights into their role during the green synthesis of AgNPs. Terpenoid compounds, including sesquiterpenes and diterpenes, are known to contain functional groups capable of donating electrons, thereby facilitating the reduction of Ag^+ ions to metallic silver [8]. In addition to their reducing capacity, these hydrophobic and oxygenated metabolites can adsorb onto the nanoparticle surface, acting as stabilizing and capping agents that prevent aggregation and contribute to colloidal stability [8, 26]. Similar roles of plant-derived terpenoids and related secondary metabolites in nanoparticle reduction and stabilization have been widely reported in green synthesis studies [8-9], supporting the dual function of the *P. pubescens* hexane extract as both a reducing and stabilizing agent in the formation of AgNPs.

Transmission Electron Microscopy (TEM) revealed silver nanoparticles (AgNPs) with heterogeneous sizes and irregular morphologies ranging from approximately 100±26.32 to 500±16.30 nm (Figure 2: A–C). Both isolated and aggregated nanoparticles were observed, indicating variability in dispersity. Similar size distributions and morphologies have been reported by Badar and coauthors [24], reinforcing the consistency of our synthesis method.

Selected Area Electron Diffraction (SAED), shown in Figure 2: D, evidenced concentric rings and bright diffraction spots, indicating the polycrystalline nature of the AgNPs. This crystallographic feature suggests the presence of well-ordered atomic planes, commonly observed in green-synthesized metallic nanoparticles.

The size, shape, and degree of aggregation of AgNPs are known to influence their antimicrobial efficacy. Nanoparticles within the 1–100 nm range exhibit a high surface-area-to-volume ratio, enhancing their interaction with bacterial membranes [25]. Although some particles in our study exceed this range, many remain within the antimicrobial-effective threshold. Aggregation may affect performance, but also reflects real-world stability patterns in phytosynthesized systems.

The antibacterial mechanism of AgNPs involves electrostatic interaction between the negatively charged bacterial membrane and the positively charged surface of the nanoparticles. This interaction promotes membrane disruption, internalization of silver ions, and subsequent oxidative stress, leading to cell death and inhibition of biofilm formation [26].

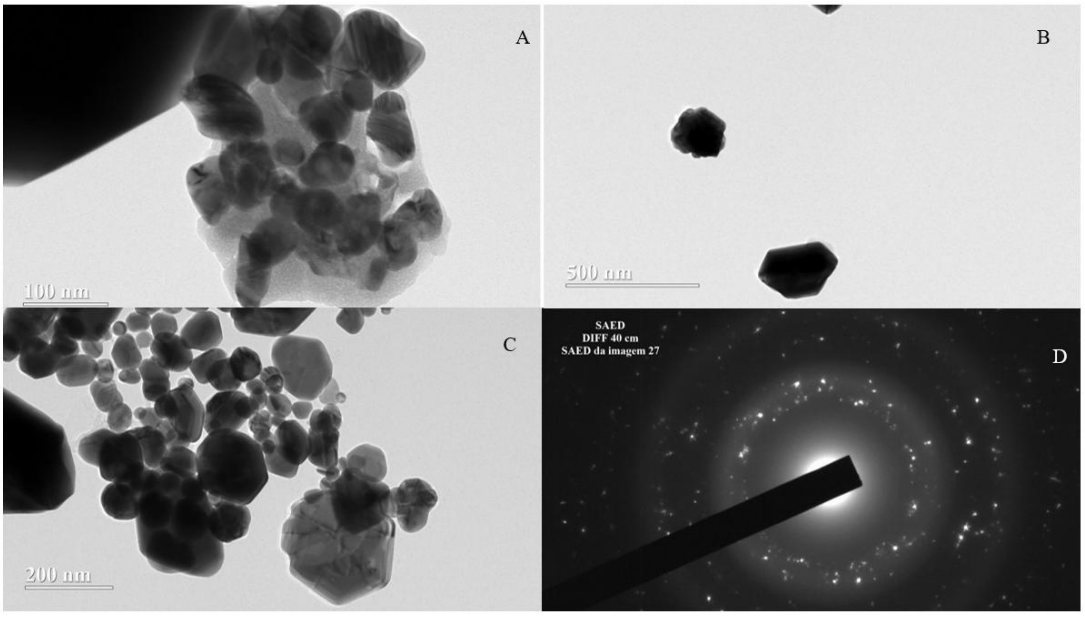

Figure 2. Transmission electron microscopy (TEM) images of silver nanoparticles (AgNPs) synthesized using hexane extract from *P. pubescens* (HE-PP). (A–C) AgNPs with irregular morphology, both dispersed and aggregated, displaying size variation from 100±26.32 to 500±16.30 nm. (D) Selected Area Electron Diffraction (SAED) pattern corresponding to image (C), indicating the polycrystalline nature of the nanoparticles.

Figure 3 displays the FTIR spectra comparing the HE-PP extract and the synthesized AgNPs. A clear decrease in transmittance intensity was observed in the broad O–H stretching band (~3.400–2.400 cm^{-1}), indicating involvement of hydroxyl-containing phytochemicals in the reduction and stabilization of AgNPs. A slight reduction in the C–H stretching vibration (~2.900 cm^{-1}) was also observed, along with a shift in the C=C stretching band from ~1.700 to ~1.600 cm^{-1}, suggesting chemical modifications during the synthesis process.

According to Santos and coauthors [1] and Miranda and coauthors [27], HE-PP contains abundant hydroxylated terpenoids such as dehydroabietol, (*E*,*E*)-farnesol, spathulenol, *Z*-linalool oxide, and *E*-geranylgeraniol, all of which contribute to the reduction of silver ions. The decreased O–H signal supports their participation as reducing agents. Additionally, the reduction in intensity of π- and δ-bonded C=C bands, likely from germacrene, β-elemene, and allo-aromadendrene, indicates their partial oxidation during nanoparticle formation. Characteristic shifts and intensity reductions in O–H, C–H, and C=C stretching bands confirm the involvement of phytochemicals as reducing and stabilizing agents during nanoparticle formation [28]. Together, TEM, SAED, and FTIR analyses confirm that the bioactive phytochemicals in HE-PP not only mediate the reduction of silver ions, but also contribute to the morphological and crystallographic properties of the resulting nanoparticles.

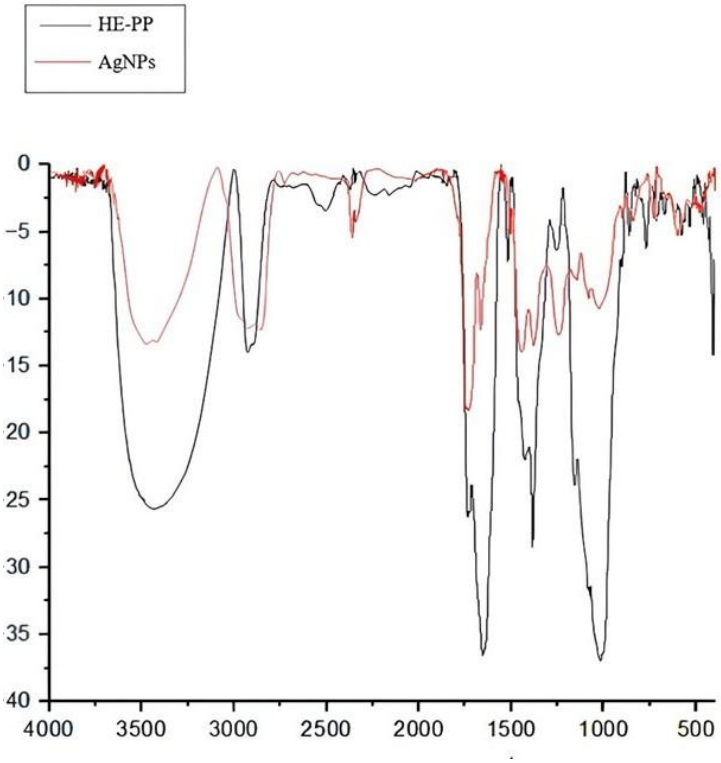

Figure 3. Fourier-transform infrared spectroscopy (FTIR) spectra comparing the hexane extract from *P. pubescens* seeds (HE-PP) and the synthesized silver nanoparticles (AgNPs).

The physicochemical analysis of HE-PP-mediated silver nanoparticles (AgNPs) revealed characteristics compatible with stable, bioactive nanomaterials, aligning with green synthesis standards reported in the literature.

Dynamic Light Scattering (DLS) measurements showed a mean hydrodynamic diameter of 187.4 ± 12.6 nm, with a polydispersity index (PDI) of 0.234, suggesting a moderately narrow size distribution. The hydrodynamic diameter obtained by DLS was noticeably larger than the particle size estimated from electron microscopy images, which is an expected and well-documented methodological difference. While electron microscopy provides information on the core size of dried nanoparticles, DLS measures the hydrodynamic diameter of particles dispersed in solution, encompassing the metallic core, the organic capping layer derived from plant metabolites, and the surrounding solvation shell. Consequently, the larger size values obtained by DLS reflect the colloidal behavior of the AgNPs in suspension rather than an increase in the metallic core dimension. These values are consistent with other green-synthesized AgNPs using plant extracts, such as those reported by Suman and coauthors (2013) [14], who observed sizes between 150 and 250 nm for *Morinda citrifolia*-based nanoparticles with similar PDI values. Although the hydrodynamic size obtained via DLS is larger than the dry size measured by TEM (100–500 nm), this discrepancy is expected due to the hydration layer and surface-bound phytochemicals influencing DLS measurements [29].

The zeta potential of the AgNPs was –31.6 ± 1.4 mV, indicating electrostatic repulsion sufficient to ensure colloidal stability. According to Mulenos [30], zeta potentials above ±30 mV are generally considered indicative of good stability in nanoparticle suspensions [30]. The HE-PP-mediated AgNPs remained visually stable for at least 30 days, without significant sedimentation or agglomeration, suggesting favorable long-term dispersion stability under ambient conditions.

The synthesis yield was estimated at 82.3%, calculated gravimetrically after drying and isolating the nanoparticles. This high efficiency demonstrates the effectiveness of the bio-reduction process mediated by *P. pubescens* phytochemicals and is comparable to yields reported for other green synthesis systems using terpenoid-rich plant extracts, such as *Euphorbia wallichii* [31].

Elemental analysis by EDX confirmed the presence of silver (Ag) as the predominant element (88.7% w/w) in the nanoparticle composition, along with signals of carbon (7.4%) and oxygen (3.9%), attributed to organic moieties derived from the plant extract. These results are in line with observations by Badar & Khan (2020), who reported similar elemental profiles in biosynthesized AgNPs stabilized by secondary plant metabolites [24]. Supporting this, ICP-OES analysis quantified the total silver content in the colloidal suspension at 18.4 ± 1.2 mg/mL, providing a robust benchmark for future *in vivo* dosing and application trials.

Together, these findings support the hypothesis that HE-PP phytoconstituents act not only as reducing agents but also as stabilizers, producing colloidally stable, chemically consistent silver nanoparticles. The combination of small to moderate hydrodynamic size, monodispersity, strong zeta potential, and high yield aligns with the prerequisites for biomedical and agricultural applications, especially in the context of antimicrobial therapy. Furthermore, the stability of the particles over extended periods without the addition of synthetic surfactants underscores the ecological and functional advantages of this green synthesis strategy.

The HE-PP-mediated silver nanoparticles (AgNPs) demonstrated notable antibacterial activity against a panel of periodontopathogenic bacterial strains, as presented in Table 1. The minimum inhibitory concentrations (MICs) for most strains (e.g., *P. anaerobius*, *A. naeslundii*, *P. gingivalis*, *P. nigrescens*, and *A. actinomycetemcomitans*) were uniformly 3.90 µg/mL, indicating broad-spectrum efficacy at low concentrations. The exception was *B. fragilis*, which exhibited a higher MIC of 15.62 µg/mL, suggesting a comparatively reduced sensitivity to the AgNPs.

Table 1. Minimum inhibitory concentration (MIC±standard deviations) of HE-PP-mediated AgNPs against periodontopathogenic bacteria.

	Bacterial strains – MIC (µg/mL)					
	P. anaerobius	*A. naeslundii*	*P. gingivalis*	*P. nigrescens*	*B. fragilis*	*A. actinomycetemcomitans*
HE-PP-mediated AgNPs	3.90±0.10	3.90±0.15	3.90±0.20	3.90±0.15	15.62±0.30	3.90±0.12
Chlorhexidine*	0.115±0.01	1.47±0.25	1.47±0.25	5.90±0.15	5.9±0.15	0.115±0.01

*Positive control

When compared to the positive control, chlorhexidine, the nanoparticles showed comparable or superior efficacy against several strains. For example, the MIC of chlorhexidine for *P. gingivalis* and *P. nigrescens* was 1.47 and 5.90 µg/mL, respectively, both higher than the 3.90 µg/mL observed for HE-PP-mediated AgNPs. Additionally, *A. actinomycetemcomitans* and *P. anaerobius* were inhibited by both agents at 3.90 and 0.115 µg/mL, respectively, further supporting the antimicrobial potential of the nanoparticles.

When compared to MIC values reported in the literature for other AgNP systems, the results obtained in this study indicate significantly enhanced antimicrobial efficacy. For instance, Zorraquín-Peña and coauthors [32] reported MICs of 24.6 µg/mL for *P. gingivalis* and *F. nucleatum* using glutathione-stabilized AgNPs, while green-synthesized AgNPs tested by Ghabban and coauthors [33] displayed MICs of 10.6 µg/mL and 13.3 µg/mL against *Streptococcus mutans* and *Actinomyces viscosus*, respectively. In a study by Halkai and coauthors [34], biosynthesized AgNPs inhibited *P. gingivalis* biofilms at a concentration of 30 µg/mL. Compared to these values, the HE-PP-mediated AgNPs exhibited a 3- to 8-fold increase in antibacterial potency. These results suggest a synergistic effect between the silver core and the bioactive phytochemicals from *P. pubescens*, reinforcing the potential of this formulation as an efficient antimicrobial agent in the control of periodontopathogenic bacteria.

The HE-PP-mediated silver nanoparticles (AgNPs) exhibited consistent antimycobacterial activity, with minimum inhibitory concentrations (MICs) of 7.80 µg/mL against all tested strains: *M. tuberculosis* (ATCC 27294), *M. avium* (ATCC 25291), and *M. kansasii* (ATCC 12478). While these MIC values are higher than those observed for the standard drug isoniazid (ranging from 0.125 to 0.50 µg/mL – Table 2), they are still within the range considered promising for alternative antimycobacterial agents, especially those derived from natural products or nanomaterials.

Table 2. Antimycobacterial activity of HE-PP-mediated AgNPs (MIC = µg/mL±standard deviations)

Bacterial strains	HE-PP-mediated AgNPs	*Isoniazid
Mycobacterium avium (ATCC 25291)	7.80±0.70	0.25±0.15
Mycobacterium kansasii (ATCC 12478)	7.80±0.50	0.50±0.15
Mycobacterium tuberculosis (ATCC 27294)	7.80±0.30	0.125±0.15

*Positive control

In the context of nanotechnology-based antimycobacterial strategies, previous studies have reported varying MIC values for AgNPs, typically depending on particle size, surface modification, and synthesis method [35]. For instance, Barua and coauthors [36] revised and reported some MIC values ranging from 12.50 to 100 µg/mL for AgNPs against *M. tuberculosis* clinical isolates using AgNPs. In this regard, the MIC of 7.80 µg/mL reported herein represents a notably enhanced activity and with a value compatible with that described by Agarwal and coauthors [37]. These data suggest that the phytochemicals present in *P. pubescens* may act synergistically with the silver core, improving membrane permeability and increasing oxidative stress in mycobacterial cells [38]. Given the rising incidence of drug-resistant mycobacterial infections and the limited efficacy of existing antimycobacterial agents, especially against atypical strains such as *M. avium* and *M. kansasii*, the present findings support a preliminary and promising action of HE-PP-mediated AgNPs.

HE-PP-mediated AgNPs exhibited strong antibacterial activity against three *X. citri* strains with differing copper resistance profiles (copper-resistant, copper-tolerant, and copper-sensitive), all presenting a minimum inhibitory concentration (MIC) of 0.48 µg/mL. In comparison, streptomycin showed variable efficacy, with MICs of 0.1844 µg/mL for the copper-resistant strain (*X. citri* 1647), 0.7375 µg/mL for the copper-tolerant strain (*X. citri* 1733), and 0.0461 µg/mL for the copper-sensitive strain (*X. citri* 12) – Table 3. These findings indicate that HE-PP-mediated AgNPs maintain consistent antimicrobial effectiveness regardless of the strain's copper resistance phenotype, highlighting their potential as alternative agents for the management of *X. citri* infections.

Table 3. Anti-*Xanthomonas citri* activity of HE-PP-mediated AgNPs, results expressed as MIC in µg/mL±standard deviations.

Bacterium	HE-PP-mediated AgNPs	Streptomycin*
Xanthomonas citri 1647 (copper-resistant)	0.48±0.01	0.1844±0.03
Xanthomonas citri 1733 (copper-tolerant)	0.48±0.01	0.7375±0.02
Xanthomonas citri 12 (copper-sensitive)	0.48±0.01	0.0461±0.05

*Positive control

HE-PP-mediated AgNPs demonstrated a remarkably consistent MIC of 0.48 µg/mL against three *X. citri* strains (copper-resistant, copper-tolerant, and copper-sensitive), indicating robust antibacterial activity that is largely independent of copper resistance mechanisms. This is notably more effective than the concentration range employed in the study by Arif and coauthors (2022), where biologically synthesized AgNPs from *Euphorbia wallichii* leaf extract was tested against *X. axonopodis*, a closely related citrus pathogen, across a dilution series ranging from 1000 to 15.62 µg/mL [31]. In addition, although MIC tests with HE-PP alone were not repeated in the present study, previous work using the same extract preparation reported MIC values of 12.50–500 µg/mL against oral pathogens and 12.50 µg/mL against *X. citri* [1]. When compared to the MICs obtained here for HE-PP-mediated AgNPs (0.48–3.90 µg/mL), these data indicate a strong synergistic enhancement of antibacterial activity.

Mechanistic insights from proteomic analysis of *X. campestris* treated with 32 µM AgNPs revealed significant modulation of proteins related to metal ion homeostasis, membrane integrity, and metabolism, thus supporting the hypothesis that AgNPs disrupt multiple cellular targets beyond simple membrane damage [39]. Furthermore, proteomic data in *Phytopathogenic Xcc* demonstrated extensive proteome changes when treated with AgNPs compared to $AgNO_3$, implying that nanoparticle-specific properties contribute to their heightened antibacterial potency [39]. These findings align with our observation of equal efficacy across strains with varying copper resistance, suggesting that silver nanoparticles overcome typical resistance barriers via multifaceted mechanisms. Additionally, comparative studies on AgNPs synthesized from green sources showed that particles smaller than 10–20 nm tend to exhibit stronger antibacterial effects, which likely explains the potent activity observed at low MIC values in our work [40]. Overall, the MIC values of HE-PP-mediated AgNPs fall well below the internationally accepted threshold of 10 µg/mL, which is commonly used to classify compounds or formulations as highly active against bacterial targets. According to Ríos and Recio (2005), MIC values below 10 µg/mL, and ideally under 2 µg/mL, are considered indicative of promising antimicrobial candidates, particularly in natural product research and pharmaceutical development [41]. Similarly, recent studies on silver nanoparticles confirm that MIC values under this threshold reflect potent antimicrobial efficacy, especially against phytopathogens and multi-resistant bacterial strains (i.e. MICs of 3.90–7.80 µg/mL); effective activity at 5–50 µg/mL against *X. oryzae* [42].

HE-PP-mediated AgNPs demonstrated a MIC of 25 µg/mL against *Helicobacter pylori*, placing them in the moderate activity category when compared to literature reports of more potent nanoparticle formulations. For instance, silver ultra-nanoclusters (SUNCs) with sizes <5 nm exhibited much stronger efficacy, with MICs of 18.14 mg/L (~18 µg/mL), and remarkably low MICs in the range of 0.16–0.33 µg/mL when combined with metronidazole, or about two orders of magnitude more effective than our AgNPs [43]. Another green-synthesized AgNP formulation derived from *Peganum harmala* seeds (average diameter ~15 nm) displayed significant activity similar to conventional antibiotics, although exact MIC values were not provided; therapeutic clearance *in vivo* was achieved with oral doses of 16 mg/kg [44].

In contrast, AgNPs synthesized via *Solanum xanthocarpum* fruit extract produced strong urease inhibitory activity (i.e. 64% inhibition at 16 µM), suggesting antibacterial potency through enzymatic interference rather than reduced cell viability alone [45]. Additionally, biogenic AgNPs have been shown to impair *H. pylori* biofilm formation and induce reactive oxygen species and DNA fragmentation, along with mitochondrial apoptosis in co-cultured mammalian cells [46]. Thus, while our observed MIC of 25 µg/mL is higher than those reported for ultra-small AgNPs or metallo-pharmaceutical hybrids, it still aligns with the activity range of many bio-derived AgNPs and retains relevance to future studies *in vivo*. Lastly, the literature underscores the importance of green synthesis of nanoparticles and highlights their promising antibacterial potential, encouraging further exploration of eco-friendly nanomaterials for biomedical applications [47].

It is important to note that silver nitrate ($AgNO_3$) was not included as a control in the present antibacterial assays. This choice was based on the primary objective of the study, which was to evaluate the antibacterial performance of green-synthesized AgNPs as colloidal nanostructures stabilized by plant-derived metabolites, rather than to compare different silver precursors. Nevertheless, extensive literature reports have demonstrated that $AgNO_3$ typically exhibits rapid but less sustained antibacterial effects, often associated with higher cytotoxicity due to the immediate release of Ag^+ ions [25,26,38]. In contrast, AgNPs are known to act as reservoirs of silver ions, providing a more controlled and prolonged antimicrobial effect, while the presence of organic capping agents from plant extracts can further modulate ion release and enhance biocompatibility [25,26,38]. Therefore, although a direct experimental comparison was not performed, the observed antibacterial activity is consistent with previously reported AgNP-mediated mechanisms rather than the sole action of free silver ions.

The cytotoxicity of HE-PP-mediated AgNPs toward a normal human fibroblast cell line was evaluated, as shown in Figure 4. The treatments exhibited statistically significant reductions in cell viability at concentrations greater than or equal to 62.50 µg/mL, yielding an IC_{50} value of 62.56 ± 3.38 µg/mL. Notably, this concentration is higher than the minimum inhibitory concentrations (MICs) determined for the tested bacterial strains, which ranged from 0.48 to 25 µg/mL. These results indicate a favorable selectivity profile, with antibacterial effects occurring at concentrations lower than those associated with cytotoxicity in host cells. Although these findings suggest good preliminary biocompatibility, further studies using additional cell models are required to confirm the safety and broader biological applicability of these nanoparticles.

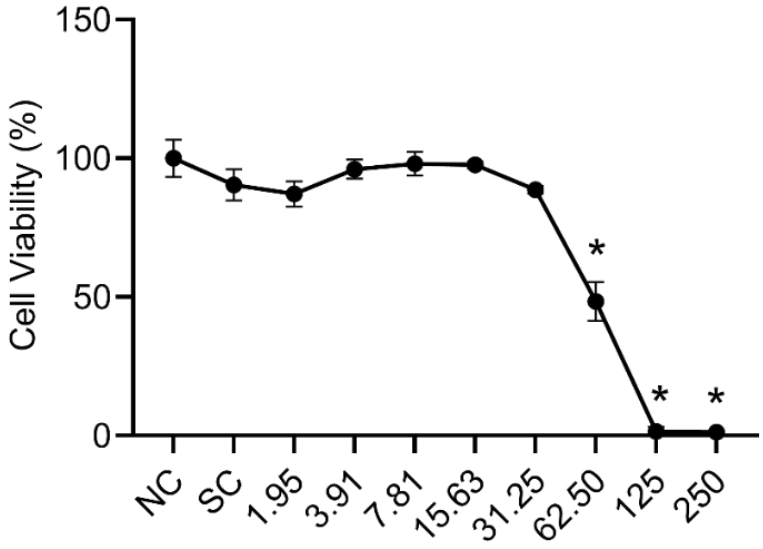

Figure 4. Percentage of cell viability obtained in culture of human fibroblasts (GM07492A cells) treated with different concentrations of HE-PP-mediated AgNPs. NC – Negative control, SC – Solvent control (1% DMSO), IC_{50} = 62.56 ± 3.38 µg/mL. *Significantly different from the negative control (p<0.05).

Taken together, the antibacterial and biocompatibility results presented in this study indicate that HE-PP-mediated AgNPs combine physicochemical stability, broad-spectrum antibacterial activity, and favorable selectivity toward mammalian cells—key attributes for their prospective use in biomedical materials. In this context, recent advances in nanomaterial engineering have demonstrated that surface-functionalized nanostructures and biocompatible nanofibrous systems can play a crucial role in biomedical applications, particularly in the prevention of post-operative complications. Advanced fabrication strategies, such as the *in situ* growth of robust superlubricated nano-skins on electrospun nanofibers and the development of engineered lubricative lecithin-based electrospun nanofibers, have been successfully applied to biomedical surfaces to prevent post-operative adhesion, highlighting the versatility and translational potential of engineered nanomaterials [48–49]. Overall, despite distinct fabrication approaches, these studies highlight the increasing importance of nanoscale design in improving biomedical performance and support future investigations into the integration of eco-friendly silver-based nanomaterials, such as those developed herein, into functional biomedical surfaces.

CONCLUSION

In conclusion, the green synthesis of silver nanoparticles (AgNPs) using *P. pubescens* seed hexane extract proved to be an effective strategy for generating stable nanomaterials with broad-spectrum antibacterial activity. The HE-PP-mediated AgNPs showed promising selectivity toward bacterial cells over normal human fibroblasts. While the findings highlight their translational relevance as alternative antimicrobial agents, further studies are needed to assess *in vivo* biosafety, pharmacokinetics, long-term biocompatibility, and environmental impact. Overall, this study advances phytochemical-mediated nanotechnology and identifies *P. pubescens* as a sustainable source for the development of bioactive nanomaterials.

Author Contributions: Conceptualization, J.G.S. and M.L.D.M.; methodology, J.G.S., C.C.F. and A.J.; software, M.R.S.M.; validation, J.G.S., C.H.G.M. and D.C.T.; formal analysis, J.G.S. and C.C.F.; investigation, J.G.S., C.C.F., A.J., M.B.S. and C.H.G.M.; resources, M.L.D.M.; data curation, J.G.S. and M.R.S.M.; writing—original draft preparation, J.G.S. and M.L.D.M.; writing—review and editing, J.G.S., C.C.F., A.J., M.B.S., C.H.G.M., M.R.S.M., D.C.T. and M.L.D.M.; visualization, M.B.S. and M.R.S.M.; supervision, M.L.D.M.; project administration, J.G.S. and A.J.; funding acquisition, C.C.F. and A.J. All authors have read and agreed to the published version of the manuscript. Please turn to the CRediT taxonomy for the term explanation. Authorship must be limited to those who have contributed substantially to the work reported.

Funding: The authors would like to thank IF Goiano – *Campus* Rio Verde, FAPEG, CNPq, and CAPES for their financial support.

Institutional Review Board Statement: Not applicable for studies not involving humans or animals.

Informed Consent Statement: Not applicable for studies not involving humans.

Data Availability Statement: The data presented in this study are available in the article.

Acknowledgments: We express our gratitude to the laboratories that contributed with essential analyses: the Multiuser High-Resolution Microscopy Laboratory at the Federal University of Goiás (LabMic/UFG), the Central Analytical Laboratory of the Physics course at the Federal University of Jataí (UFJ), and IFGOIANO-*Campus* Rio Verde.

Conflicts of Interest: The authors declare no conflicts of interest. Funders had no role in the study design; in the collection, analyses or interpretation of data; in writing the manuscript, nor in the decision to publish the results.

Use of Generative Artificial Intelligence

The authors declare that no generative artificial intelligence (AI) or AI-assisted technologies were used to generate or modify the scientific content of this manuscript, including the conception of the study, data collection, data analysis, interpretation of results, or creation of original text, figures, tables or graphical abstracts, apart from routine tools for spelling, grammar checking and reference management that do not create original scholarly content.

REFERENCES

1. Dos Santos JG, Fernandes CC, Silva NB, Calefi GG, Martins CH, Volpini GA, et al. Volatile compounds of hexane extract from *Pterodon pubescens* Benth seeds and its significant *in vitro* potential against different bacterial strains. Nat Prod Res. 2023 Mar; 39(5): 1428-3.
2. Pereira MF, Martino T, Dalmau SR, Paes MC, Barja-Fidalgo C, Albano RM, et al. Terpenic fraction of *Pterodon pubescens* inhibits nuclear factor kappa B and extracellular signal-regulated protein Kinase 1/2 activation and deregulates gene expression in leukemia cells. BMC Complement Alter Med. 2012 Nov; (12): 1-8.

3. Nucci C, Mazzardo-Martins L, Stramosk J, Brethanha LC, Pizzolatti MG, Santos AR, et al. Oleaginous extract from the fruits *Pterodon pubescens* Benth induces antinociception in animal models of acute and chronic pain. J Ethnopharmacol. 2012 Aug; 143(1)1: 170-8.
4. Nucci-Martins C, Martins DF, Nascimento LF, Venzke D, Oliveira AS, Frederico MJ, et al. Ameliorative potential of standardized fruit extract of *Pterodon pubescens* Benth on neuropathic pain in mice: Evidence for the mechanisms of action. J Ethnopharmacol. 2015 Dec; (175): 273-6.
5. Lloret F, Santos CCJ, Medina LS, Queiroz NCA, Sousa IMO, Ruiz ALTG, et al. [6α-acetoxy-7α-hydroxy-vouacapan isolated from *Pterodon pubescens* Benth. fruits with selective activity against prostate cancer cell lines: artifact or natural product?] Med Aromat Plants, 2016 Jun; (5)238.
6. Basting RT, de Oliveira Sousa IM, Butterweck V, Foglio MA. Antiproliferative effects of *Pterodon pubescens* extract and isolated diterpenes in HaCaT cells. Planta Med. 2021 Mar; 87(03): 218-4.
7. Souza VHDS, Basting RT, Sousa IMDO, Queiroz NDCA, Carvalho JED, Foglio MA. Evaluation of non-clinical toxicity of extract and vouacapans from fruits of *Pterodon pubescens* Benth. Drug and Chem. Toxicol. 2022 May; 45(3): 1325-8.
8. Vanlalveni C, Lallianrawna S, Biswas A, Selvaraj M, Changmai B, Rokhum SL. Green synthesis of silver nanoparticles using plant extracts and their antimicrobial activities: A review of recent literature. RSC Advances. 2021 Jan; 11(5): 2804-7.
9. Fahim M, Shahzaib A, Nishat N, Jahan A, Bhat TA, Inam A. Green synthesis of silver nanoparticles: A comprehensive review of methods, influencing factors, and applications. JCIS Open. 2024 Dec; 100125.
10. Batalini C, Stocco LO, da Silva Fernandes RT, Junior JM. Phytochemical, phytothoxic and antifungal evaluations of stem bark of *Pterodon pubescens* Benth (sucupira branca). Braz. J. Develop. 2020 Oct; 6(10): 77589-7.
11. Andrade PMD, Melo DCD, Alcoba AET, Ferreira WG, Pagotti MC, Magalhães LG, et al. Chemical composition and evaluation of antileishmanial and cytotoxic activities of the essential oil from leaves of *Cryptocarya aschersoniana* Mez. (Lauraceae Juss.). An Acad Bras Ciênc. 2018 Sep; 90(3): 2671-8.
12. Adams RP. Identification of essential oil components by gas chromatography/mass spectrometry. Allured Publ Crop Carol Steam, IL. 2007.
13. Jiang T, Huang J, Peng J, Wang Y, Du L. Characterization of Silver Nanoparticles Synthesized by the Aqueous Extract of *Zanthoxylum nitidum* and Its Herbicidal Activity against *Bidens pilosa* L. Nanomaterials. 2023 May;13(10):1637.
14. Suman TY, Rajasree SR, Kanchana A, Elizabeth SB. Biosynthesis, characterization and cytotoxic effect of plant mediated silver nanoparticles using *Morinda citrifolia* root extract. Colloids Surf B Biointerfaces. 2013;106:74-8.
15. Rizwana H, Alzahrani T, Alwahibi MS, Aljowaie RM, Aldehaish HA, Alsaggabi NS, et al. Phytofabrication of silver nanoparticles and their potent antifungal activity against phytopathogenic fungi. Processes. 2022;10(12):2558.
16. dos Santos JG, Fernandes CC, Macedo AS, Santos AL, Ribeiro AB, Esperandim TR, et al. Bioactivities of hexane extracts from different parts of *Cochlospermum regium* (Schrank) Pilg. and their volatile compositions. J Biol Active Prod Nature. 2025 Apr; 15(2): 156-4.
17. Ribeiro AMR, Fernandes CC, de Paula Menezes, de Oliveira AM, Gonçalves DS, Martins CHG, et al. Antibacterial screening of hexane extracts from *Psidium myrtoides,* a Brazilian native plant. Ciênc Nat. 2024;(46):e84178-e8.
18. Quintino RL, Reis AC, Fernandes CC, Martins CHG, Colli AC, Crotti AEM, et al. Brazilian green propolis: chemical composition of essential oil and their *in vitro* antioxidant, antibacterial and antiproliferative activities. Braz Arch Biol Technol. 2020 Oct; 63, e20190408.
19. Riss TL, Moravec RA, Niles AL, Duellman S, Benink, HA, Worzella TJ, et al. Cell viability assays. Assay guidance manual, 2016.
20. Giarola LR, Coco JC, de Oliveira Sousa IM, Cefali LC, Ataide JA, Tavares GD, et al. *Pterodon pubescens* Benth (sucupira) microencapsulation influence on formulation stability outcome compared to non-encapsulated extract. J Drug Deliv Sci Tech. 2022 Jan; 67, 102875.
21. Masuda Y, Nakaya M, Aiuchi T, Hashimoto S, Nakajo S, Nakaya K. The mechanism of geranylgeraniol-induced apoptosis involves activation, by a caspase-3-like protease, of a c-Jun N-terminal kinase signaling cascade and differs from mechanisms of apoptosis induced by conventional chemotherapeutic drugs. Leuk Res. 2000 Nov; 24(11): 937-0.
22. Oliveira LA, Oliveira GA, Borges LL, Bara MTF, Silveira D. Vouacapane diterpenoids isolated from *Pterodon pubescens* and their biological activities. R Bras Farmacogn. 2017 Oct; (27): 663-2.
23. Oselusi SO, Sibuyi NR, Meyer M, Madiehe AM. Phytonanotherapeutic applications of plant extract-synthesized silver nanoparticles in wound healing—a prospective overview. BioNanoScience. 2024 Jul; 14(3): 3455-5.
24. Badar W, Ullah Khan MA. Analytical study of biosynthesised silver nanoparticles against multi-drug resistant biofilm-forming pathogens. IET Nanobiotechnol. 2020 Jun; 14(4): 331-40.
25. Ozdal M, Gurkok S. Recent advances in nanoparticles as antibacterial agent. ADMET and DMPK. 2022 Feb; 10(2): 115-9.
26. Mikhailova EO. Silver nanoparticles: Mechanism of action and probable bio-application. J. Funct. Biomat. 2020 Nov; 11(4): 84.
27. Miranda MLD, Garcez FR, Abot AR, Garcez WS. Sesquiterpenes and other contituents from leaves of *Pterodon pubescens* Benth (Leguminosae). Quim. Nova. 2014 Jun; 37: 473-6.

28. Pasieczna-Patkowska S, Cichy M, Flieger J. Application of Fourier Transform Infrared (FTIR) Spectroscopy in Characterization of Green Synthesized Nanoparticles. Molecules. 2025 Feb; 30(3): 684.
29. Geraldes AN, Rosero WAA, Rostelato MECM, Sarkis JES. Calculation of the Budget of Uncertainty on Measurements Size Nanoparticles Using Dynamic Light Scattering. J Braz Chem Soc. 2024 Mar; 35(8): e-20240039
30. Mulenos MR, Lujan H, Pitts LR, Sayes CM. Silver Nanoparticles Agglomerate Intracellularly Depending on the Stabilizing Agent: Implications for Nanomedicine Efficacy. Nanomaterials 2020 Sep; 10: 1953.
31. Arif M, Ullah R, Ahmad M, Ali A, Ullah Z, Ali M, et al. Green Synthesis of Silver Nanoparticles Using *Euphorbia wallichii* Leaf Extract: Its Antibacterial Action against Citrus Canker Causal Agent and Antioxidant Potential. Molecules 2022 May;27:3525.
32. Zorraquín-Peña I, Cueva C, González de Llano D, Bartolomé B, Moreno-Arribas MV. Glutathione-stabilized silver nanoparticles: antibacterial activity against periodontal bacteria, and cytotoxicity and inflammatory response in oral cells. Biomedicines. 2020 Sep; 8(10): 375.
33. Ghabban H, Alnomasy SF, Almohammed H, Al Idriss OM, Rabea S, Eltahir Y. Antibacterial, cytotoxic, and cellular mechanisms of green synthesized silver nanoparticles against some cariogenic bacteria (*Streptococcus mutans* and *Actinomyces viscosus*). J Nanomat. 2022 Feb; 2022(1): 9721736.
34. Halkai KR, Halkai R, Mudda JA, Shivanna V, Rathod V. Antibiofilm efficacy of biosynthesized silver nanoparticles against endodontic-periodontal pathogens: An: *in vitro*: study. J Conserv Dent End. 2018 Dec; 21(6): 662-6.
35. Sati A, Ranade TN, Mali SN, Ahmad Yasin HK, Pratap A. Silver nanoparticles (AgNPs): comprehensive insights into bio/synthesis, key influencing factors, multifaceted applications, and toxicity─ a 2024 update. ACS Omega. 2025 Feb; 10(8): 7549-2.
36. Barua N, Buragohain AK. Therapeutic Potential of Silver Nanoparticles (AgNPs) as an Antimycobacterial Agent: A Comprehensive Review. Antibiotics. 2024 Nov; 13(11): 1106.
37. Agarwal P, Mehta A, Kachhwaha S, Kothari SL. Green synthesis of silver nanoparticles and their activity against *Mycobacterium tuberculosis*. Adv Sci Eng Med. 2023 May; 5(7): 709-4.
38. Godoy-Gallardo M, Eckhard U, Delgado LM, de Roo Puente YJ, Hoyos-Nogués M, Gil FJ, et al. Antibacterial approaches in tissue engineering using metal ions and nanoparticles: From mechanisms to applications. Bioactive Materials. 2021 May; 6(12): 4470-0.
39. Santos IR, Ribeiro DG, Mendes PDN, Fontes W, Luz IS, Silva LP, et al. Biotechnological potential of silver nanoparticles synthesized by green method to control phytopathogenic bacteria: contributions from a proteomic analysis. Braz J Microbiol. 2024 Dec; 55(4): 3239-0.
40. Tian Y, Luo J, Wang H, Zaki HE, Yu S, Wang X, et al. Bioinspired green synthesis of silver nanoparticles using three plant extracts and their antibacterial activity against rice bacterial leaf blight pathogen *Xanthomonas oryzae* pv. oryzae. Plants. 2022 Oct; 11(21): 2892.
41. Rios JL, Recio MC. Medicinal plants and antimicrobial activity. J Ethnopharmacol. 2005 Aug; 100(1-2): 80-4.
42. Mishra S, Yang X, Ray S. Antibacterial and biofilm inhibition activity of biofabricated silver nanoparticles against *Xanthomonas oryzae* pv. *oryzae* causing blight disease of rice instigates disease suppression. World J Microbiol Biotechnol. 2020 Mar; 36(55).
43. Grande R, Sisto F, Puca V, Carradori S, Ronci M, Aceto A, et al. Antimicrobial and antibiofilm activities of new synthesized silver ultra-nanoclusters (SUNCs) against *Helicobacter pylori*. Front Microbiol. 2020 Jul;11:1705.
44. Amin M, Hameed S, Ali A, Anwar F, Shahid SA, Shakir I, et al. Green synthesis of silver nanoparticles: structural features and *in vivo* and *in vitro* therapeutic effects against *Helicobacter pylori* induced gastritis. Bioinorg Chem Appl. 2014 Aug; 2014(1):135824.
45. Amin M, Anwar F, Janjua MRSA, Iqbal MA, Rashid U. Green Synthesis of Silver Nanoparticles through Reduction with *Solanum xanthocarpum* L. Berry Extract: Characterization, Antimicrobial and Urease Inhibitory Activities against *Helicobacter pylori.* Int J Mol Sci. 2012 Aug; 13(8): 9923-1.
46. Gurunathan S, Jeong JK, Han JW, Zhang XF, Park JH, Kim JH. Multidimensional effects of biologically synthesized silver nanoparticles in *Helicobacter pylori*, *Helicobacter felis*, and human lung (L132) and lung carcinoma A549 cells. Nanoscale Res Lett. 2015 Feb 5:10:35.
47. Numan K, Sajjad AS, Muhammad H, Sidra TM, Ibrar K, Azam H, et al. Synthesis, characterization, and antibacterial activities of SnO and SnO@$FeCl_2$ nanoparticles using *Olea europaea* subsp. Africana (Mill.) P.S. Green mediated green. CyTA – J. Food, 2025 Jan; 23:1, 2421787.
48. Wang Yi, Xu Y, Zhai W, Zhang Z, Liu Y, Cheng S, et al. In-situ growth of robust superlubricated nano-skin on electrospun nanofibers for post-operative adhesion prevention. Nat Commun. 2022 Aug; 13:1, 5056.
49. Li J, Lin H, Li J, Wang Y. Engineered Lubricative Lecithin-Based Electrospun Nanofibers for the Prevention of Postoperative Abdominal Adhesion. Pharmaceutics, 2024 Dec; 16:1, 1562.